

## Percolation of interacting diffusing particles

Robin Blumberg Selinger and H. Eugene Stanley

*Center for Polymer Studies and Department of Physics, Boston University, Boston, Massachusetts 02215*

(Received 2 October 1989)

We explore the connectivity properties of diffusing particles with short-range interactions for dimensions  $d = 1, 2$ . We consider both “blind” and “myopic” diffusion rules (for the blind case, the walker chooses the next step from among *all* neighbor sites while in the myopic case the walker chooses from among only the unblocked sites). We show that—for all  $d$ —the equilibrium state of a system of particles diffusing according to the blind rule, at density  $\rho$ , is equivalent to the lattice gas with interaction parameter  $J = 0$  and chemical potential  $\mu = 2 \sinh^{-1} \{ [(2\rho - 1)^2 / 4\rho(1 - \rho)]^{1/2} \}$ . The connectivity properties of the blind diffusion system are described by random site percolation in all dimensions. The myopic diffusion system is more complicated. For  $d = 1$ , the equilibrium state of a system of particles diffusing according to the myopic rule, with particle density  $\rho$ , is equivalent to a lattice gas with  $J = -\ln(2)$  and  $\mu = \ln(2) + 2 \sinh^{-1} \{ [(2\rho - 1)^2 / 2\rho(1 - \rho)]^{1/2} \}$ . Also, for  $d = 1$ , the number of clusters of size  $s$  is approximately  $n_s = \rho p_{\text{eff}}^{s-1} (1 - p_{\text{eff}})^2$ , where  $p_{\text{eff}} \leq \rho$ . An approximation for  $p_{\text{eff}}$  is given that agrees closely with Monte Carlo simulations. For  $d = 2$ , the myopic diffusion system has no mapping to the lattice-gas model. Rather, it undergoes a percolation transition at a threshold density  $\rho_c$ . On the square lattice,  $\rho_c = 0.617 \pm 0.004$ , a value that is higher than the threshold for random site percolation. However, percolation and myopic diffusion appear to be in the same universality class.

### I. INTRODUCTION

Percolation is the paradigm model for all forms of connectivity. In its original form, percolation is a static model, in which particles are positioned according to some rule. The simplest rule is random placement, but more complicated rules have also been discussed.

In nature, particles often get where they are by some natural process such as diffusion. In this paper we address the following question. What are the percolation properties of a system whose particles get where they are by *diffusion*?

At first sight, since diffusion is random, one might expect that the same statistical distribution will arise as for the original version of percolation; a snapshot of the system would reveal clusters described by random site percolation, with an infinite connected cluster present if and only if the density of atoms is at or above the percolation threshold. However if the particles interact—even by an innocuous hard-core repulsion—then the foundation for this intuition breaks down. The “rules” by which the atoms diffuse can introduce spatial correlations in the positions of the atoms. We shall find, in fact, that quite different connectivity phenomena occur depending on the form of the interaction. Even as small a change as that between “blind” and “myopic” diffusion is found to have a marked effect (for the blind case, the walker chooses the next step from among *all* neighbor sites while in the myopic case the walker chooses from among only the unblocked sites).

Diffusion of interacting particles is certainly of more than mere academic interest because of its application to diffusion of atoms in adsorbed monolayers and interstitial and substitutional alloys.<sup>1,2</sup> Much work has also been motivated by the study of ionic conduction.<sup>3</sup> Kehr,

Kutner, and Binder have investigated diffusion in three dimensional lattice gases with both attractive and repulsive interactions.<sup>4</sup> Diffusion of particles has also been studied in the case where motion is restricted to a fractal substrate.<sup>5</sup> The connectivity properties of interacting diffusing particles were addressed by Sapoval and co-workers<sup>6</sup> who investigated the geometry of “diffusion fronts.” Coniglio<sup>7</sup> and Coniglio and Klein<sup>8</sup> examined the connectivity properties of the Ising model in the study of correlated or interacting percolation. This problem was also addressed by Muller-Krumbhaar.<sup>9</sup>

The “stirred percolation” model of conduction in a microemulsion<sup>10</sup> is closely related to the present work. In that model, blind random walkers representing droplets of water diffuse on a lattice, and the sites unoccupied by walkers represent oil. Thus the model system has both spatial and temporal disorder. Several researchers have investigated diffusion of a generalized excitation confined to the water region of the lattice.<sup>11</sup> In this paper, we shall instead investigate the percolation properties of the system, e.g. the cluster size distribution of the water droplets, and show that they are altered if the droplets diffuse by myopic, rather than blind, rules.

The dynamic percolation model of Druger, Nitzan, and Ratner<sup>12</sup> also addresses the issue of diffusion in a medium with both spatial and temporal disorder. In that model, a particle diffuses on a bond lattice. A transition probability  $\omega_i$ , chosen randomly from a probability distribution, is assigned to each bond  $i$ . The transition probabilities are “renewed,” or generated randomly again, periodically with a characteristic time scale  $\tau_{\text{ren}}$ . The present work is in some sense an example of dynamic percolation, where the transition probabilities are determined not from a probability distribution but via a diffusion process.

Our model is defined as follows. On a  $d$ -dimensional hypercubic lattice of linear size  $L$ , each site is occupied by a particle with probability  $\rho$ . Then, one particle is selected at random and attempts to take a step according to a diffusion rule to be defined below. Then another particle is selected, attempts to take a step, and this process is repeated indefinitely. Periodic boundary conditions are employed to minimize edge effects. One time unit is defined as the time in which  $\rho L^d$  particles are selected, so that on average each particle has taken one step. In this process, each particle executes a random walk whose trajectory depends on the environment. A cluster is defined as in site percolation, such that two particles on nearest-neighbor sites are said to belong to the same cluster. The system reaches equilibrium when many successive "snapshots" of the system show that quantities such as the mean-square cluster size have attained stable values.

We focus on two diffusion rules: the "blind" and "myopic" rules invented by Mitescu and Roussenq<sup>13</sup> in their study of random walks on percolation clusters. Consider a particle situated on a lattice of coordination number  $z$ . According to the blind rule, the particle first chooses one of the  $z$  possible directions, and if the

nearest-neighbor site in that direction is unblocked, the particle moves there; otherwise it stays where it was. Let  $\omega(i \rightarrow j)$  be the transition probability per unit time from site  $i$  to nearest-neighbor site  $j$ . Then  $\omega(i \rightarrow j) = 1/z$  for  $j$  unblocked, and  $\omega(i \rightarrow i) = b_i/z$  where  $b_i$  is the number of blocked nearest-neighbor sites. Transition probabilities for a blind particle in several configurations are shown in Fig. 1(a).

According to the myopic rule, the particle chooses among the *unblocked* directions with equal probability, and if all directions are blocked, it does not move. Thus,  $\omega(i \rightarrow j) = 1/u_i$  for  $j$  unblocked, where  $u_i$  is the number of unblocked neighbor sites. If  $u_i > 0$ ,  $\omega(i \rightarrow i) = 0$ , and if  $u_i = 0$ ,  $\omega(i \rightarrow i) = 1$ . Transition probabilities for a myopic particle in several configurations are shown in Fig. 1(b).

Majid *et al.*<sup>14</sup> showed that in an exact enumeration calculation of diffusion on percolation clusters, the blind rule leads to faster convergence of the diffusion properties to their scaling laws. However, they showed that aside from this difference in convergence time, the two rules lead to the same scaling behavior.

We address a different problem. How do the connectivity properties of particles diffusing on a lattice depend on the choice of blind or myopic rules? We start by examining the nature of the two rules. Both the blind and myopic diffusion rules contain a hard core repulsion, for in both cases two particles are never allowed to reside on the same lattice site. The myopic rule, however, has an additional repulsion, which may be seen by examining the equilibrium probability distribution of a single particle on a one-dimensional lattice with *fixed* barriers.<sup>15</sup> Consider the one-dimensional lattice shown in Fig. 2. The sites marked with an  $x$  are occupied by fixed barriers. The equilibrium probability distribution  $P(i)$  may be found by solving the discrete equation

$$P(i) = P(i-1)\omega(i-1 \rightarrow i) + P(i+1)\omega(i+1 \rightarrow i) + P(i)\omega(i \rightarrow i). \tag{1}$$

Plugging in the blind rule values for the transition probabilities  $\omega(i \rightarrow j)$  yields the solution  $P(i) = \text{constant}$  for all unblocked sites  $i$ , as shown in Fig. 2(a). In fact, it may be shown that for the blind rule, Eq. (1) is a discretized version of the diffusion equation in equilibrium,  $d^2P/dx^2 = 0$  with reflecting boundary conditions at the barriers implying that  $dP/dx = 0$  at barriers.<sup>16</sup>

Plugging in the myopic rule values for the transition probabilities  $\omega(i \rightarrow j)$  yields a different solution;  $P(i)$  is

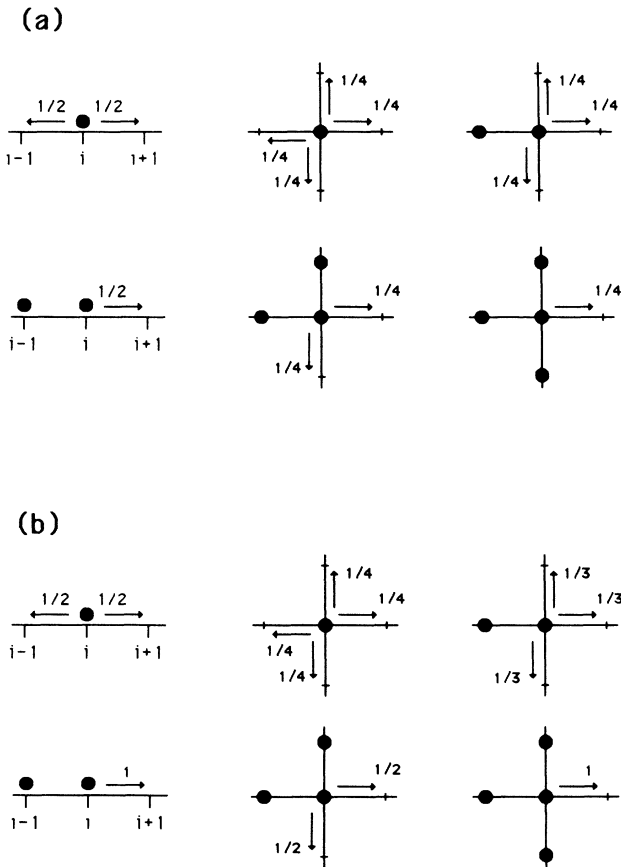


FIG. 1. (a) Examples of the blind diffusion rule in one and two dimensions. The transition probabilities  $\omega(i \rightarrow j)$  are shown for one walker in each configuration. Where the probabilities sum to less than unity, there is a finite probability for the particle to stay at the same site. (b) As above, for the myopic rule.

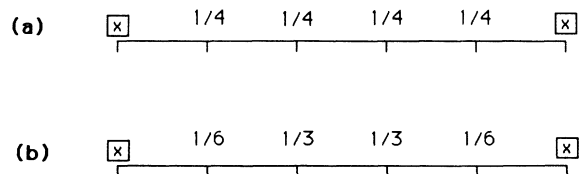


FIG. 2. A one-dimensional lattice with fixed barriers marked as  $\times$ , with the equilibrium probability density of a single particle, according to (a) the blind rule, and (b) the myopic rule.

constant on all sites away from the barriers, and half that value on sites next to the barriers, as shown in Fig. 2(b). That is, myopic particles have a strong repulsion from the barriers.

## II. CONNECTION TO THE ONE-DIMENSIONAL LATTICE GAS

Here we demonstrate that the equilibrium state of a one-dimensional system of particles diffusing according to the blind rule is equivalent to the lattice gas with interaction parameter  $J=0$ . We also show that such a system with the myopic rule is equivalent to the lattice gas with  $J=-\ln(2)$ . The lattice gas Hamiltonian may be written

$$-\beta\mathcal{H}=J\sum_i\sigma_i\sigma_{i+1}+\mu\sum_i\sigma_i, \quad (2)$$

where  $\sigma_i=0$  or 1 is the number of particles at site  $i$ . Here  $\mu$  is a chemical potential,  $\beta$  is the reduced temperature, and  $J$  is an interaction parameter. For  $J>0$  lattice gas particles tend to clump together, and for  $J<0$  they tend to stay apart, in analogy with ferromagnetic and antiferromagnetic interactions in the Ising model.

To demonstrate the connections discussed above, we show that the dynamics imposed by the blind and myopic rules satisfy the detailed balance condition for the lattice gas with  $J=0$  and  $J=-\ln(2)$ , respectively. Detailed balance implies that for any two states 1 and 2 of the system,

$$x_1R(1\rightarrow 2)=x_2R(2\rightarrow 1), \quad (3)$$

where  $R(i\rightarrow j)$  is the rate of transition from state  $i$  to state  $j$ , and  $x_i$  is the weight of state  $i$ .

Consider two states of the one-dimensional system of size 4 with periodic boundary conditions, shown in Fig. 3. For the blind rule, the probability of a transition from state 1 to state 2 in a single step is

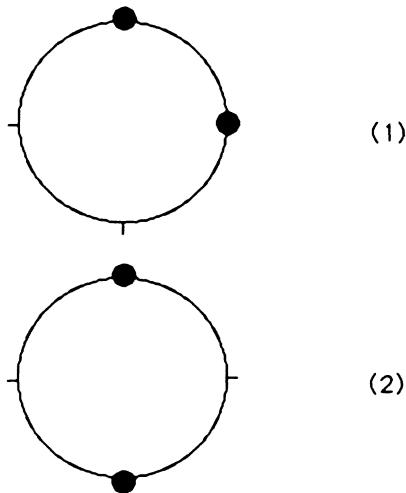


FIG. 3. A one-dimensional lattice of size 4 with periodic boundary conditions, with two particles. Two possible states are shown.

$$R(1\rightarrow 2)=\frac{1}{2}\times\frac{1}{2}=\frac{1}{4}, \quad (4)$$

because first the particle on the right is chosen with probability  $\frac{1}{2}$ , and it steps to the bottom site with probability  $\frac{1}{2}$ . Similarly, the probability of a transition from 2 to 1 is

$$R(2\rightarrow 1)=\frac{1}{2}\times\frac{1}{2}=\frac{1}{4}, \quad (5)$$

because the particle on the bottom is chosen with probability  $\frac{1}{2}$ , and it steps to the site on the right with probability  $\frac{1}{2}$ . Thus, detailed balance implies that

$$\frac{x_1}{x_2}=\frac{R(2\rightarrow 1)}{R(1\rightarrow 2)}=1. \quad (6)$$

The lattice gas in equilibrium has, for these two states,

$$\frac{x_1}{x_2}=\frac{e^{2\mu+J}}{e^{2\mu}}. \quad (7)$$

The quantities in Eqs. (6) and (7) agree if  $J=0$ . Thus, the blind rule obeys the detailed balance condition for the lattice gas with  $J=0$ , at least in this simple example. More complicated examples yield the same result.

For the myopic rule, we find that

$$R(1\rightarrow 2)=\frac{1}{2}\times 1=\frac{1}{2}, \quad (8)$$

because the particle on the right is chosen with probability  $\frac{1}{2}$  and moves to the bottom site with probability 1. The reverse transition has the rate

$$R(2\rightarrow 1)=\frac{1}{2}\times\frac{1}{2}=\frac{1}{4}, \quad (9)$$

because the particle on the bottom is chosen with probability  $\frac{1}{2}$  and steps to the right with probability  $\frac{1}{2}$ . Thus we find

$$\frac{x_1}{x_2}=\frac{R(2\rightarrow 1)}{R(1\rightarrow 2)}=\frac{1}{2}. \quad (10)$$

This result agrees with the lattice gas value in Eq. (7) with  $J=-\ln(2)$ . Again, more complicated examples yield the same result.

We note that both blind and myopic rules conserve particle number, as particles are never created or removed from the system. The comparisons made above were for fixed particle number. In general, the density in the lattice gas model is not fixed, but is determined by  $J$  and  $\mu$ . In one dimension, the average density  $\rho$  in a lattice gas is

$$\rho=\frac{1}{2}\left[1+\frac{\sinh\left[\frac{\mu+J}{2}\right]}{\left[e^{-J}+\sinh^2\left[\frac{\mu+J}{2}\right]\right]^{1/2}}\right]. \quad (11)$$

This result comes from the exact solution of the magnetization of the Ising model in one dimension, with suitable transformations to the lattice gas model.<sup>17</sup> This relation completes the connection between the blind and myopic diffusion systems and the lattice gas, in one dimension. Inverting Eq. (11) and plugging in appropriate values of

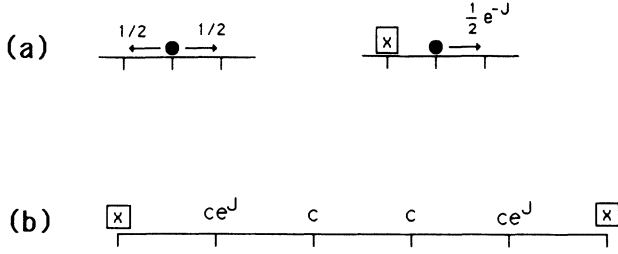


FIG. 4. For the general interaction rule, (a) transition probabilities, and (b) equilibrium probability density of a single particle on a lattice with fixed barriers.

$J$ , we find that a one-dimensional system of particles at density  $\rho$  diffusing according to the blind rule is equivalent to the one-dimensional lattice gas with

$$J=0, \quad \mu = 2 \sinh^{-1} \left[ \left( \frac{(2\rho-1)^2}{4\rho(1-\rho)} \right)^{1/2} \right]. \quad (12)$$

A one-dimensional system of particles at density  $\rho$  diffusing according to the myopic rule is equivalent to a one-dimensional lattice gas with

$$J = -\ln(2), \quad (13)$$

$$\mu = \ln(2) + 2 \sinh^{-1} \left[ \left( \frac{(2\rho-1)^2}{2\rho(1-\rho)} \right)^{1/2} \right].$$

We note that in one dimension, both the blind and myopic diffusion rules are special cases of a more general interaction rule with tunable strength  $J$ . Under the general rule, a particle with no occupied neighbor sites has probability  $\frac{1}{2}$  to move to each neighbor site. A particle with two occupied neighbor sites has probability 1 to stay where it is. A particle with one unoccupied neighbor site has probability  $\frac{1}{2}e^{-J}$  to move to the unoccupied neighbor site, and probability  $1 - \frac{1}{2}e^{-J}$  to stay at the same site. These transition probabilities are shown in Fig. 4(a). The parameter  $J$  may take values in the range  $[-\ln 2, \infty]$ . The blind rule corresponds to  $J=0$ , while the myopic rule corresponds to  $J=-\ln 2$ . As the notation suggests, the strength  $J$  of the interaction is the same as the interaction parameter  $J$  of the equivalent lattice gas. This equivalence may be demonstrated by detailed balance arguments like those given above. The equilibrium probability density of a single particle on a lattice with fixed barriers is shown in Fig. 4(b).

### III. PERCOLATION PROPERTIES: ONE DIMENSION

Because blind rule diffusion is equivalent to the noninteracting lattice gas, its percolation properties are described by random site percolation<sup>18</sup> because the density at neighboring sites is uncorrelated. Myopic rule diffusion cannot be described by random site percolation, however, because neighboring sites are correlated. We performed Monte Carlo simulations of myopic rule diffusion, and calculated the cluster distribution  $n_s(\rho)$ ,

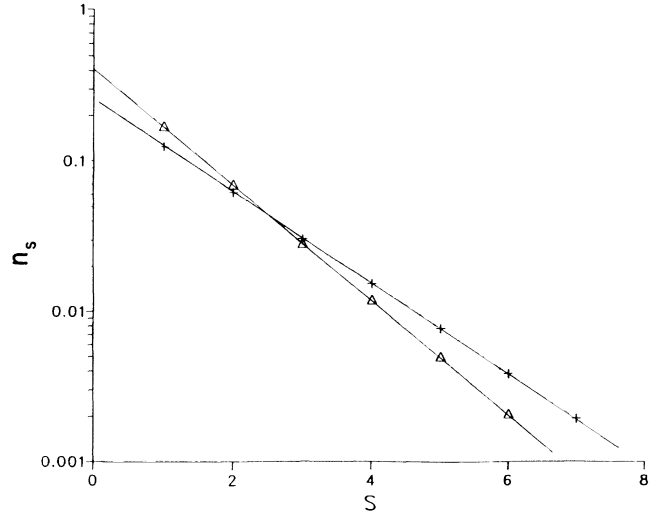


FIG. 5. The cluster size distribution  $n_s$  for the myopic diffusion system in one dimension at density  $\rho=0.5$  ( $\Delta$ ). Shown for comparison is the same quantity for random site percolation with  $\rho=0.5$  (+).

the number of clusters of size  $s$ . A typical cluster distribution is shown in Fig. 5, along with the cluster distribution for random site percolation at the same density. For random site percolation, at density  $\rho$ , the cluster distribution is given by

$$n_s = \rho^s (1-\rho)^2. \quad (14)$$

For the myopic system in one dimension, we find instead

$$n_s \sim p_{\text{eff}}^s, \quad (15)$$

where  $p_{\text{eff}} \leq \rho$ . That is, the cluster distribution drops off faster with increasing  $s$  than in random site percolation at the same density, and therefore there are more small clusters. Normalization  $\sum_s s n_s = \rho$  implies that the full expression for  $n_s$  is

$$n_s = \rho (1-p_{\text{eff}})^2 p_{\text{eff}}^{s-1}. \quad (16)$$

An estimate of  $p_{\text{eff}}$  can be made by taking advantage of the analogy with the lattice gas. The quantity  $p_{\text{eff}}$  is the average density on a site with one neighbor that is definitely occupied. Because the interaction is antiferromagnetic,  $p_{\text{eff}}$  is normally smaller than  $\rho$ . The approximate value is found by considering the configurations shown in Fig. 6 with the weights indicated. Site 1 is occupied with probability 1, and site 3 is occupied with probability  $\rho$ . Then  $p_{\text{eff}}$  is the average density on site 2. The result for the lattice gas is

$$p_{\text{eff}} = \frac{\rho e^{\mu+2J} + (1-\rho)e^{\mu+J}}{\rho + (1-\rho) + \rho e^{\mu+2J} + (1-\rho)e^{\mu+J}}. \quad (17)$$

Plugging in the correct values of  $J$  and  $\mu$  for the myopic diffusion system given in Eq. (13) gives a prediction for  $p_{\text{eff}}$  as a function of  $\rho$ :

$$p_{\text{eff}} = \frac{2-\rho}{4e^{\mu} + 2 - \rho}, \quad (18a)$$

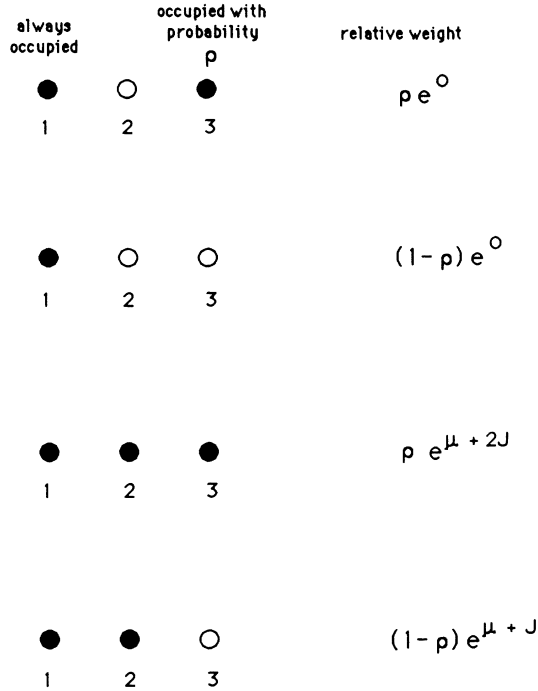


FIG. 6. Configurations considered in the approximation of  $p_{\text{eff}}$ , shown with their respective weights. The quantity  $p_{\text{eff}}$  is the probability that site 2 is occupied, given that site 1 is occupied with probability 1, and site 3 is occupied with probability  $\rho$ . The energy used in the weight factor thus depends only on site 2 and its bonds.

with

$$\mu = \ln(2) + 2 \sinh^{-1} \left[ \left( \frac{(2\rho - 1)^2}{2\rho(1-\rho)} \right)^{1/2} \right]. \quad (18b)$$

This estimate of  $p_{\text{eff}}$  versus  $\rho$  is plotted in Fig. 7, along with values from Monte Carlo simulations of both the myopic system and the equivalent lattice gas. The agreement is surprisingly good. This agreement reflects the fact that the lattice gas correlation length is short, and therefore next-nearest-neighbor sites are nearly uncorrelated. A better estimate of  $p_{\text{eff}}$  can be found by enumerating the configurations on a system of length 4, where site 1 is occupied with probability 1 and site 4 is occupied with probability  $\rho$ , and weighting each configuration as above.

#### IV. PERCOLATION PROPERTIES: TWO DIMENSIONS

As mentioned above, the connectivity properties of the blind rule diffusion system are described by random site percolation. This result holds in all dimensions; the detailed balance argument given in Eqs. (3)–(7) may be extended to any dimension with the same result,  $J=0$ . However, the myopic rule diffusion system is more complicated, because the detailed balance argument that gave  $J=-\ln(2)$  in one dimension cannot be extended to higher dimensions. In fact, there is no mapping to the

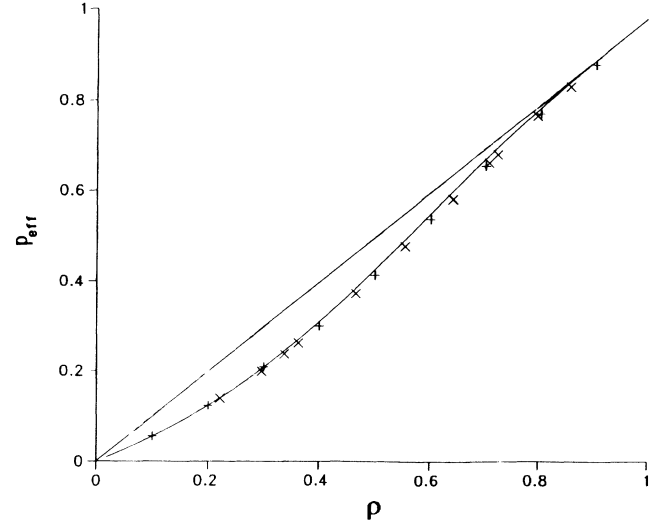


FIG. 7. A comparison of the prediction for  $p_{\text{eff}}$  given in Eq. (18) (lower solid curve) with simulation results from (+) one-dimensional myopic rule diffusion, and (x) the equivalent lattice gas. Agreement is best for  $\rho \ll 1$ . Shown also is the straight line  $p_{\text{eff}} = \rho$ .

lattice gas in two dimensions for any value of  $J$ . For this reason, we cannot use our knowledge of the lattice gas to determine the connectivity properties of the myopic rule diffusion system in two dimensions.

Instead, we perform Monte Carlo simulations of myopic rule diffusion on the square lattice. To determine that the system has reached equilibrium, we wait until the mean square cluster size has reached a stable value, typically a few or up to ten Monte Carlo time steps.<sup>19</sup> Then we take “snapshots” of the system once per Monte Carlo time step and analyze the cluster distribution. Lattice sizes used range from  $L=10$  to  $L=200$ . A sample configuration for  $L=20$  and density  $\rho=0.5$  is shown in Fig. 8, along with a random site percolation configuration with density  $p=0.5$ . The myopic diffusion configuration appears to have more small clusters, which reflects the “anticorrelation” induced by the myopic rule.

We find that the myopic rule gives rise to anticorrelated site percolation with a percolation transition at  $\rho_c = 0.617 \pm 0.004$  on the square lattice, a value which is definitely higher than the random site percolation threshold  $p_c = 0.59275$ .<sup>18</sup> Thus the anticorrelation imposed by the myopic rule increases the percolation threshold. Intuitively, the threshold is higher for particles that repel one another since the threshold is determined by the linking together of “blobs” by strings of singly connected sites (“red sites”)—any repulsion among the sites serves to render even more fragile these strings.<sup>20</sup>

It is difficult to accurately estimate critical exponents from Monte Carlo simulations in small systems. However, we attempt to show that our simulation results are consistent with the critical exponents of random site percolation. We calculate two exponents:  $\nu$  and  $\gamma$ . We define  $\pi(\rho)$  as the fraction of equilibrium configurations

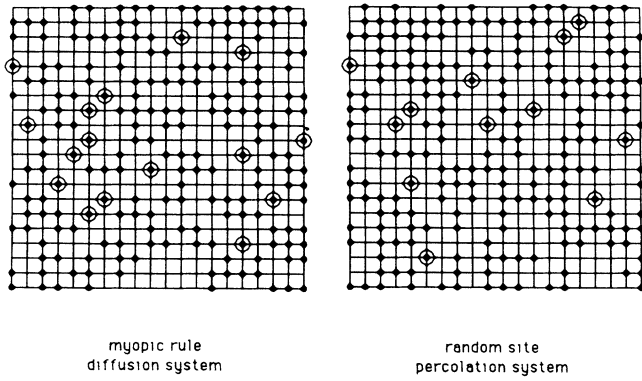


FIG. 8. Small sample configurations of the myopic diffusion system with  $L=20$  and  $\rho=0.5$ , and random site percolation with  $p=0.5$ . Clusters of size 1 are circled, with periodic boundary conditions used. The myopic diffusion system appears to have more small clusters than the random site percolation system.

that have a spanning cluster at a given particle density  $\rho$ . (A spanning cluster must reach from the upper boundary of the lattice to the lower, with periodic boundary conditions connecting only the right and left boundaries.) In Fig. 9  $\pi(\rho)$  is plotted for system sizes  $L=10, 20, 40, 80$ , and  $160$ . As  $L$  increases,  $\pi(\rho)$  approaches a step function. We define  $\rho_{20}$  and  $\rho_{80}$  as the particle densities at which 20% and 80% of configurations span;<sup>21</sup> these quantities are plotted in Fig. 10. From finite size scaling theory,<sup>22</sup> we expect

$$\rho_{20}(\infty) - \rho_{20}(L) \sim L^{1/\nu}, \quad \rho_{80}(L) - \rho_{80}(\infty) \sim L^{1/\nu'}, \quad (19)$$

where  $\nu$  and  $\nu'$  refer to the connectedness length singularity above and below  $\rho_c$ , respectively, and  $\rho_{20}(\infty)$

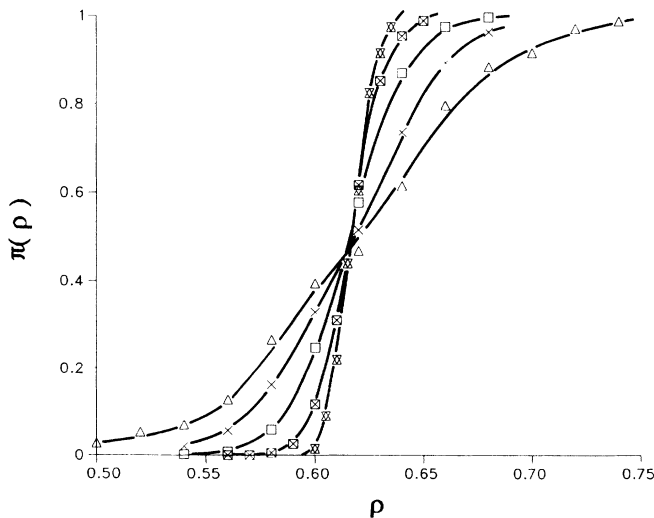


FIG. 9. Shown is  $\pi(\rho)$  for  $(\Delta)L=10$ ,  $(\times)L=20$ ,  $(\square)L=40$ ,  $(\otimes)L=80$ , and  $(\boxtimes)L=160$ . The approach to a step function with increasing  $L$  can be seen.

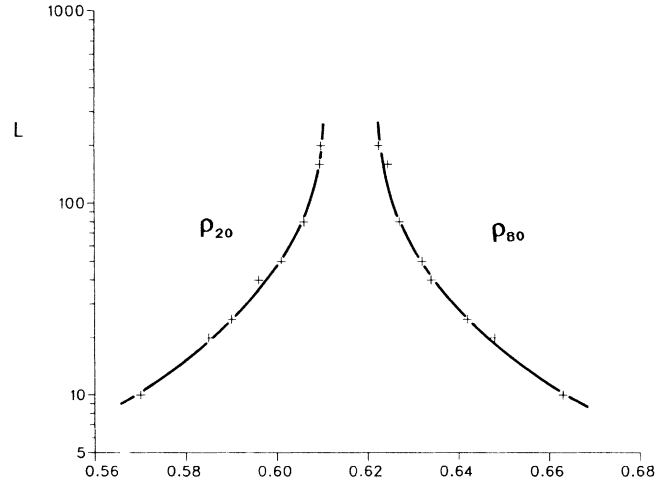


FIG. 10. A plot of system size  $L$  vs  $\rho_{20}(L)$  and  $\rho_{80}(L)$ .

$=\rho_{80}(\infty)=\rho_c$ . Choosing  $\rho_c^{\text{trial}}=0.617$  to make  $\nu=\nu'$  as closely as possible, we plot the quantities in Eq. (19) in Fig. 11. Also plotted is a straight line with slope  $-\nu=-\frac{4}{3}$ , the value for random percolation in two dimensions.<sup>18</sup> While agreement is not exact, one may conclude that the somewhat scattered data are at least consistent with this value. This method of measuring  $\nu$  however has the drawback that  $\rho_c$  must be known. Another method is to plot  $L$  versus  $\rho_{80}(L) - \rho_{20}(L)$ , as shown in Fig. 12. Again, the scatter is large. Shown for comparison is a straight line with slope  $-1.4$ . We conclude that for the myopic rule diffusion system  $\nu=1.4 \pm 0.1$ , which is consistent with the random percolation value  $\nu=\frac{4}{3}$ .

Better agreement, however, is found for the exponent describing the divergence of the mean square cluster size  $S(\rho) \equiv \langle s^2 n_s \rangle$ . This quantity scales as<sup>18</sup>

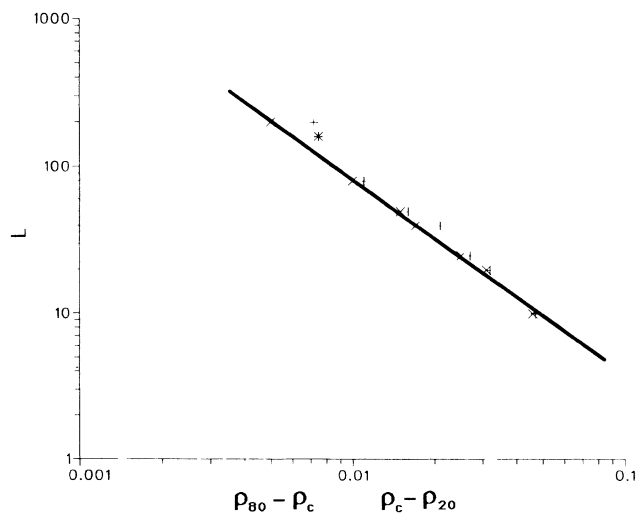


FIG. 11. Shown is system size  $L$  vs  $\rho_c - \rho_{20}$  and  $\rho_{80} - \rho_c$ . The value of  $\rho_c$  was chosen in order to make the two lines as close to parallel as possible.

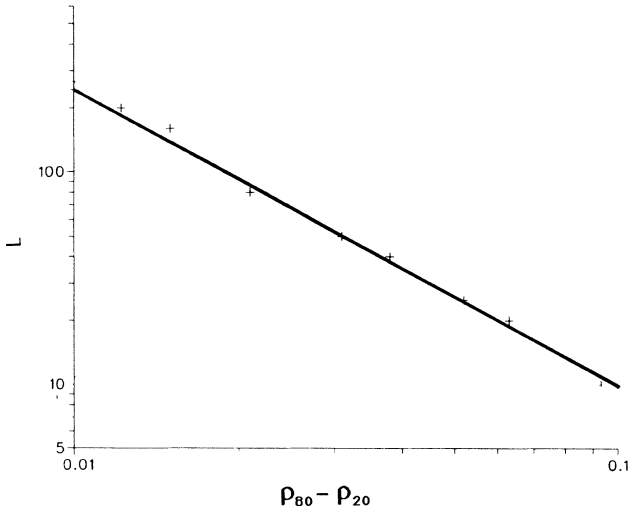


FIG. 12. A plot of system size  $L$  vs  $\rho_{80}(L) - \rho_{20}(L)$ . Shown also is a line with slope  $-1.4$ .

$$S(\rho) \sim \begin{cases} C_+ (\rho - \rho_c)^{-\gamma} & \rho < \rho_c \\ C_- (\rho_c - \rho)^{-\gamma'} & \rho > \rho_c. \end{cases} \quad (20)$$

$S(\rho)$  versus  $|\rho - \rho_c|$  is plotted in Fig. 13, with  $\rho_c = 0.617$ . Shown also are straight lines with slope  $\gamma = \frac{43}{18}$ , the value for random percolation in two dimensions.<sup>18</sup> Here the simulation results appear to agree very well with this value. Thus we have found no indication that myopic rule diffusion in two dimensions is in a different universality class than random site percolation.

## V. CONCLUSION

We examined the connectivity properties of systems of diffusing, interacting particles with the blind and myopic diffusion rules. We find that the blind rule case is equivalent to the lattice gas with  $J=0$  in all dimensions. Because the density on neighboring sites is uncorrelated, the connectivity properties of blind rule diffusion are described by random site percolation. The myopic case in one dimension is equivalent to the lattice gas with parameters  $J$  and  $\mu$  as given in Eq. (13). Because the lattice gas correlation length is short when  $J$  is small, we can approximate the cluster distribution as  $n_s = \rho p_{\text{eff}}^{s-1} (1 - p_{\text{eff}})^2$ ,

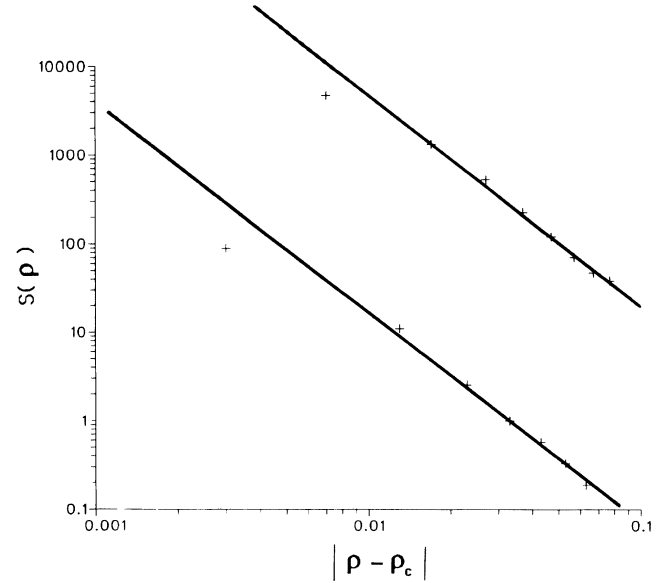


FIG. 13. A plot of mean-square cluster size  $S(\rho)$  vs  $|\rho - \rho_c|$ . Also shown are lines with slope  $-\gamma = -\frac{43}{18}$ , the exponent for random site percolation. The data appear to be consistent with this value.

where  $n_s$  is the number of clusters with  $s$  particles, and  $p_{\text{eff}} \leq \rho$  is the average density on a site next to an occupied site. An approximation for  $p_{\text{eff}}$  is given in Eq. (18), and this prediction agrees surprisingly well with Monte Carlo simulations of both myopic rule diffusion and the equivalent lattice gas. Myopic rule diffusion in two dimensions undergoes a percolation transition at a critical density  $\rho_c = 0.617 \pm 0.004$  for the square lattice, about 3% larger than for random site percolation. The exponents  $\nu$  and  $\gamma$  for this system appear to be consistent with those of random percolation in two dimensions. Thus we conclude that the two systems are in the same universality class.

## ACKNOWLEDGMENTS

We wish to thank F. Family, S. Havlin, R. Hilfer, W. Klein, R. Orbach, and J. Selinger for helpful discussions. We also thank NASA, the Link Foundation, the National Science Foundation, and the Office of Naval Research for financial support.

<sup>1</sup>K. W. Kehr and K. Binder, in *Applications of the Monte Carlo Method in Statistical Physics*, edited by K. Binder (Springer, Berlin, 1987); S. Havlin and D. Ben-Avraham, *Adv. Phys.* **36**, 695 (1987); J. W. Haus and K. W. Kehr, *Phys. Rep.* **150**, 263 (1987), and references contained therein.

<sup>2</sup>A. Bunde, S. Havlin, R. Nossal, and H. E. Stanley, *Phys. Rev. B* **32**, 3367 (1985), and references contained therein.

<sup>3</sup>W. Dieterich, P. Fulde, and I. Peschel, *Adv. Phys.* **29**, 527 (1980).

<sup>4</sup>K. W. Kehr, R. Kutner, and K. Binder, *Phys. Rev. B* **23**, 4931 (1981); R. Kutner, K. Binder, and K. W. Kehr, *ibid.* **26**, 2967

(1982); **28**, 1846 (1983).

<sup>5</sup>C. Amitrano, A. Bunde, and H. E. Stanley, *J. Phys. A* **18**, L923 (1985).

<sup>6</sup>B. Sapoval, M. Rosso, and J. F. Gouyet, *J. Phys. (Paris) Lett.* **46**, L149 (1985); see also J. F. Gouyet, M. Rosso, and B. Sapoval, *Phys. Rev. B* **37**, 1832 (1988); J. P. Hulin, E. Clement, C. Baudet, J. F. Gouyet, and M. Rosso, *Phys. Rev. Lett.* **61**, 333 (1988).

<sup>7</sup>A. Coniglio, *J. Phys. A* **8**, 1773 (1975); see also A. Coniglio, F. di Liberto, G. Monroy, and F. Perrugi, *Phys. Lett.* **87A**, 189 (1982).

- <sup>8</sup>A. Coniglio and W. Klein, *J. Phys. A* **13**, 2775 (1980).
- <sup>9</sup>H. Muller-Krumbhaar, in *Monte Carlo Methods in Statistical Physics*, edited by K. Binder (Springer, Berlin, 1979).
- <sup>10</sup>M. Laguës, *J. Phys. (Paris) Lett.* **40**, L331 (1979).
- <sup>11</sup>A. L. R. Bug and Y. Gefen, *Phys. Rev. A* **35**, 1301 (1987); G. S. Grest, I. Webman, S. A. Safran, and A. L. R. Bug, *ibid.* **33**, 2842 (1986).
- <sup>12</sup>S. D. Druger, A. Nitzan, and M. A. Ratner, *J. Chem. Phys.* **79**, 3133 (1983); S. D. Druger, M. A. Ratner, and A. Nitzan, *Phys. Rev. B* **31**, 3939 (1985); S. D. Druger and M. A. Ratner, *ibid.* **38**, 12 589 (1988).
- <sup>13</sup>C. D. Mitescu and J. Rousseny, *Ann. Israel Phys. Soc.* **5**, 81 (1983).
- <sup>14</sup>I. Majid, D. Ben-Avraham, S. Havlin, and H. E. Stanley, *Phys. Rev. B* **30**, 1626 (1984).
- <sup>15</sup>T. Vicsek, *Z. Phys. B* **45**, 153 (1981).
- <sup>16</sup>S. Chandrasekhar, *Rev. Mod. Phys.* **15**, 1 (1943), reprinted in *Noise and Stochastic Processes*, edited by N. Wax (Dover, New York, 1953).
- <sup>17</sup>R. K. Pathria, *Statistical Mechanics* (Pergamon, Oxford, 1972), p. 417. The transformation is  $J = 4J_{\text{Ising}}$ , and  $\mu = 2B_{\text{Ising}} - 4J_{\text{Ising}}$ .
- <sup>18</sup>D. Stauffer, *Introduction to Percolation Theory* (Taylor and Francis, London, 1985); see also D. Stauffer and H. E. Stanley, *From Newton to Mandelbrot: A Primer in Theoretical Physics* (Springer Verlag, Heidelberg, 1990); and D. Stauffer, in *Correlations and Connectivity: Geometrical Aspects of Physics, Chemistry and Biology*, edited by H. E. Stanley and N. Ostrowsky (Kluwer Academic, Dordrecht, 1990).
- <sup>19</sup>We plan to explore the scaling properties of the relaxation time associated with this approach to equilibrium in a future paper.
- <sup>20</sup>H. E. Stanley, *J. Phys. A* **10**, L211 (1977); A. Coniglio, *Phys. Rev. Lett.* **46**, 250 (1980).
- <sup>21</sup>Here we follow the procedure used by J. Rousseny, J. Clerc, G. Giraud, E. Guyon, and H. Ottavi, *J. Phys. (Paris)* **37**, 99 (1976); see also R. Blumberg, G. Shlifer, and H. E. Stanley, *J. Phys. A* **13**, L147 (1980).
- <sup>22</sup>M. E. Fisher, in *Critical Phenomena*, Proceedings of the Enrico Fermi Summer School, Course 51, Varenna, 1970, edited by M. S. Green (Academic, New York, 1971); A. Sur, J. L. Lebowitz, J. Marro, M. L. Kalos, and S. Kirkpatrick, *J. Stat. Phys.* **15**, 345 (1976).